

Trajectory Servoing: Image-Based Trajectory Tracking Using SLAM

Shiyu Feng^{1,†}, Zixuan Wu^{2,†}, Yipu Zhao³ and Patricio A. Vela²

Abstract—This paper describes an image based visual servoing (IBVS) system for a nonholonomic robot to achieve good trajectory following without real-time robot pose information and without a known visual map of the environment. We call it *trajectory servoing*. The critical component is a feature-based, indirect SLAM method to provide a pool of available features with estimated depth, so that they may be propagated forward in time to generate image feature trajectories for visual servoing. Short and long distance experiments show the benefits of trajectory servoing for navigating unknown areas without absolute positioning. Trajectory servoing is shown to be more accurate than pose-based feedback when both rely on the same underlying SLAM system.

I. INTRODUCTION

Navigation systems with real-time needs often employ hierarchical schemes that decompose navigation across multiple spatial and temporal scales. Doing so permits the navigation solution to respond in real-time to novel information gained from sensors, while being guided by the more slowly evolving global path. At the lowest level of the hierarchy lies trajectory tracking to realize the planned paths or synthesized trajectories. In the absence of an absolute reference (such as GPS) and of an accurate map of the environment, there are no external mechanisms to support trajectory-tracking. On-board mechanisms include odometry through *proprioceptive* sensors (wheel encoders, IMUs, etc.) or visual sensors. Pose estimation from proprioceptive sensors is not observable, thus visual sensors provide the best mechanism to anchor the robot’s pose estimate to external, static position references. Indeed visual odometry (VO) or visual SLAM (V-SLAM) solutions are essential in these circumstances. However, they too experience drift, mostly due to the integrated effects of measurement noise. Is it possible to do better?

The hypothesis explored in this paper is that *performing trajectory tracking in the image domain reduces the sensitivity of trajectory tracking systems reliant on VO or V-SLAM for accuracy*. In essence, the trajectory tracking problem is shifted from feedback in pose space to feedback in perception space. Perception space approaches have several favorable properties when used for navigation [1], [2]. Shifting the representation from being world-centric to being

viewer-centric reduces computational demands and improves run-time properties. For trajectory tracking without reliable absolute pose information, simplifying the feedback pathway by skipping processes that are not relevant to—or induce sensitivities to—the local tracking task may have positive benefits. Using imaging sensors to control motion relative to visual landmarks is known as *visual servoing*. Thus, the objective is to explore the use of image-based visual servoing for long-distance trajectory tracking with a stereo camera as the primary sensor. The technique, which we call *trajectory servoing*, will be shown to have improved properties over systems reliant on VO or V-SLAM for pose-based feedback.

A. Related Work

1) *Visual Teach and Repeat*: Evidence that visual features can support trajectory tracking or consistent navigation through space lies in the *Visual Teach and Repeat* (VTR) navigation problem in robotics [3], [4]. Given data or recordings of prior paths through an environment, robots can reliably retrace past trajectories. The teaching phase of VTR creates a visual map that contains features associated with robot poses obtained from visual odometry [3], [5]–[8]. Extensions include real-time construction of the VTR data structure during the teaching process, and the maintenance and updating of the VTR data during repeat runs [5], [6]. Feature descriptor improvements make the feature matching more robust to the environment changes [8], [9]. Visual data in the form of feature points can have task relevant and irrelevant features, which provide VTR algorithms an opportunity to select a subset that best contributes to the localization or path following task [5], [7]. While visual map construction seems similar to visual SLAM, map construction is usually not dynamic; it is difficult to construct or update visual map in real-time while in motion because of the separation of the teach and repeat phases. In addition, VTR focuses more on local map consistency and does not work toward global pose estimation [7] since the navigation problems it solves are usually defined in the local frame.

Another type of VTR uses the optical flow [4], [10] or feature sequence [11]–[13] along the trajectory, which is then encoded into a VTR data structure and control algorithm in the teaching phase. Although this method is similar to visual servoing, the system is largely over-determined. It can tolerate feature tracking failure, compared with traditional visual servo system, but may lead to discontinuities [14]. Though this method handles long trajectories, and may be supplemented from new teach recordings, it can only track taught trajectories.

*This work supported in part by NSF Award #1849333.

† Equal contribution

¹S. Feng is with the School of Mechanical Engineering and the School of Electrical and Computer Engineering, Georgia Institute of Technology, Atlanta, GA 30308, USA. shiyufeng@gatech.edu

²Z. Wu and P.A. Vela are with the School of Electrical and Computer Engineering and the Institute for Robotics and Intelligent Machines, Georgia Institute of Technology, Atlanta, GA 30308, USA. {zwu380, pvela}@gatech.edu

³Y. Zhao is with Facebook Reality Labs Research, Redmond, USA. {yipuz}@fb.com

2) *Visual Servoing*: Visual servoing (VS) has a rich history and a diverse set of strategies for stabilizing a camera to a target pose described visually. VS algorithms are classified into one of two categories: image based visual servoing (IBVS) and position based visual servoing (PBVS) [15], [16]. IBVS implementations include both feature stabilization and feature trajectory tracking [16], [17]. As a feedback strategy IBVS regulation does not guarantee what path is taken by the robot since the feature space trajectory has a nonlinear relationship with the Cartesian space trajectory of the robot. Identifying a feature path to track based on a target Cartesian space trajectory requires mapping the robot frame and the target positions into the image frame over time to generate the feature trajectory [17], [18], precisely what is done here.

The target application is trajectory tracking for a mobile robot. Mobile robots have been studied as candidates for visual servoing [3], [4], [19]–[23]. Some of them use IBVS but do not use the full IBVS equations involving the image Jacobian. The centroid of the features [3] [22], the most frequent horizontal displacement of the matched feature pairs [4] or other qualitative cost functions [21] are used to generate [3] or correct [4] the feedforward angular velocity of mobile robot. These simplifications are reasonable since the lateral displacement of the features reflects task relevant movement to be regulated by the robot. However, they are best suited to circumstances with higher inaccuracy tolerance such as an outdoor, open field navigation. We use more precise velocity relations between the robot and feature motion to generate a feedback control signal for exact tracking similar to [19]. That work studied the path reaching problem with a visible path, which does not hold here.

3) *Navigation Using Visual SLAM*: Visual simultaneous localization and mapping (V-SLAM) systems estimate the robot's trajectory and world structure as the robot moves through space [24]. For some autonomous robots, the SLAM pose estimates provide good signals for using pose-based feedback to track trajectories using standard control policies. The problem associated to reliance on SLAM is the potential to accrue large estimation drift, which degrades trajectory tracking and goal attainment.

Pose estimation accuracy of SLAM is a major area of study [25]–[29]. However, most studies only test under open-loop conditions [25]–[27], [29], i.e., they only analyze the pose estimation difference with the ground truth trajectory, and do not consider the error induced when the estimated pose informs feedback control. More recently, closed-loop evaluation of V-SLAM algorithms as part of the feedback control and navigation system are tested for individual SLAM systems [30]–[32] or across different systems [33]. Closed-loop studies expose the sensitivity of pose-based feedback control and navigation, e.g., sensitivity to V-SLAM estimation drift and latency. Our work builds upon an existing closed-loop benchmarking framework and shows sensitivity reduction over conventional pose-based closed-loop navigation solution. The proposed *trajectory servoing* (TS) method is not tied to a specific V-SLAM implementation.

B. Image-Based Visual Servoing Rate Equations

The core algorithm builds on IBVS [34], thus this section covers IBVS with an emphasis on how it directly relates the velocity of image features to the robot velocities via the image Jacobian [15], [16]. These equations will inform the trajectory tracking problem under non-holonomic robot motion. We use the more modern notation from geometric mechanics [35] since it provides equations that better connect to contemporary geometric control and SLAM formulations for moving rigid bodies.

1) Non-Holonomic Robot and Camera Kinematic Models:

Let the motion model of the robot be a kinematic Hilare robot model where the pose state $g_{\mathcal{R}}^{\mathcal{W}} \in SE(2)$ evolves under the control $u = [\nu, \omega]^T$ as

$$\dot{g}_{\mathcal{R}}^{\mathcal{W}} = g_{\mathcal{R}}^{\mathcal{W}} \cdot \begin{bmatrix} 1 & 0 \\ 0 & 0 \\ 0 & 1 \end{bmatrix} \begin{bmatrix} \nu \\ \omega \end{bmatrix} = g_{\mathcal{R}}^{\mathcal{W}} \cdot \xi_u, \quad (1)$$

for ν a forward linear velocity and ω an angular velocity, and $\xi_u \in \mathfrak{se}(2)$. The state is the robot frame \mathcal{R} relative to the world frame \mathcal{W} . The camera frame \mathcal{C} is presumed to be described as $h_{\mathcal{C}}^{\mathcal{R}}$ relative to the robot frame. Consequently, camera kinematics relative to the world frame are

$$\dot{h}_{\mathcal{C}}^{\mathcal{W}} = g_{\mathcal{R}}^{\mathcal{W}} \cdot h_{\mathcal{C}}^{\mathcal{R}} \cdot \text{Ad}_{h_{\mathcal{C}}^{\mathcal{R}}}^{-1} \cdot \begin{bmatrix} 1 & 0 \\ 0 & 0 \\ 0 & 1 \end{bmatrix} \begin{bmatrix} \nu \\ \omega \end{bmatrix} = g_{\mathcal{R}}^{\mathcal{W}} \cdot h_{\mathcal{C}}^{\mathcal{R}} \cdot \zeta_u \quad (2)$$

with $\zeta_u \in \mathfrak{se}(2)$. Now, let the camera projection equations be given by the function $H : \mathbb{R}^3 \rightarrow \mathbb{R}^2$ such that a point $q^{\mathcal{W}}$ projects to the camera point $r = H \circ h_{\mathcal{W}}^{\mathcal{C}}(q^{\mathcal{W}})$. Under camera motion, the differential equation relating the projected point to the camera velocity is

$$\dot{r} = DH(q^{\mathcal{C}}) \cdot (\zeta_u \cdot q^{\mathcal{C}}), \quad (3)$$

where the point q is presumed to be static, i.e., $\dot{q} = 0$, and $q^{\mathcal{C}} = h_{\mathcal{W}}^{\mathcal{C}} q^{\mathcal{W}}$, and D is the differential operator. Since the operation $\xi \cdot q$ is linear for $\xi \in \mathfrak{se}(2)$, $q \in \mathbb{R}^3$, it can be written as a matrix-vector product $M(q)\xi$ leading to,

$$\dot{r} = DH(q^{\mathcal{C}}) \cdot M(q^{\mathcal{C}})\zeta_u = L(q^{\mathcal{C}})\zeta_u. \quad (4)$$

where $L : \mathbb{R}^3 \times \mathfrak{se}(2)$ is the Image Jacobian. Given the point and projection pair $(q, r) \in \mathbb{R}^3 \times \mathbb{R}^2$, L works out to be

$$L(q) = L(q, r) = \begin{bmatrix} -\frac{f}{q^3} & 0 & r^2 \\ 0 & -\frac{f}{q^3} & -r^1 \end{bmatrix}, \quad (5)$$

where f is the focal length. Recall that $r = H(q)$. Re-expressing it as a function of (q, r) simplifies its written form, and exposes what information is available from the image directly $r \in \mathbb{R}^2$ and what additional information must be known to compute it: coordinate q^3 from $q^{\mathcal{C}} \in \mathbb{R}^3$ in the camera frame, which is also called depth. With a stereo camera, the depth value is triangulated. The next section will use these equations for image-based trajectory tracking.

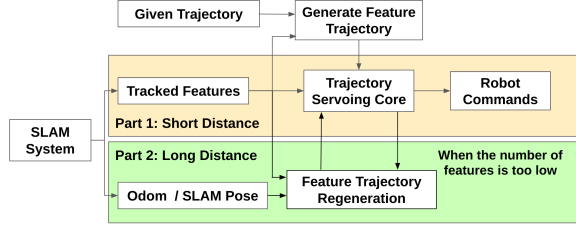


Fig. 1. A trajectory serving system has two major components. One steers the robot to track short paths, while the other ensures the sufficiency of features to use by querying a SLAM module.

II. TRAJECTORY SERVOING

A. Contributions

The system described in this paper blends visual servoing, SLAM, and basic concepts from VTR to enable trajectory tracking of feasible paths by a mobile robot in unknown environments with sufficient visual texture. We call this combination of methods *trajectory servoing* because the objective is to perform long-term trajectory tracking using visual servoing techniques. What enables this objective to be met is a stereo visual SLAM system [25], which ties the desired trajectory to the image information.

The algorithmic components and information flow of a trajectory serving system are depicted in Fig. 1, and consist of two major components. The first one, described in §II, is a trajectory serving system for a set of world points and specified trajectory. These points are obtained from the V-SLAM system as well as tracked over time. It is capable of guiding a mobile robot along short paths. The second component, described in §III, supervises the core trajectory serving system and confirms that it always has sufficient features from the feature pool to operate. Should this quantity dip too low, it queries the V-SLAM module for additional features and builds new feature tracks.

Both §II and §III include benchmarking and evaluation experiments quantifying the performance of the core trajectory serving system for short paths and the entire system for long paths. Trajectory servoing is pretty unique in that short-term trajectories can be tracked as well as pose-based feedback control with access to perfect odometry. Though long-term accuracy is undermined by the reliance on SLAM, trajectory servoing minimizes the reliance and exhibits less sensitivity to estimation error than pose feedback methods.

B. Trajectory Servoing

Pose-based feedback control is generally used in trajectory tracking. In the absence of global position knowledge, V-SLAM system provides the pose estimates needed for feedback. Tracking performance will largely depend on localization accuracy since the V-SLAM system serves as an observer of robot pose in the feedback loop. Fig. 2 shows the block diagram of the typical V-SLAM pose-based control architecture. Pose estimation is sensitive to image measurements. Any uncertainty (e.g. IMU bias, camera noise, calibration error, etc.) will accumulate [36], immediately

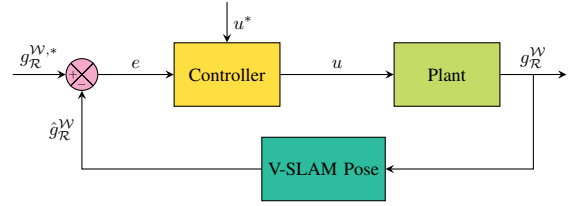


Fig. 2. Block Diagram for V-SLAM Pose Based Control

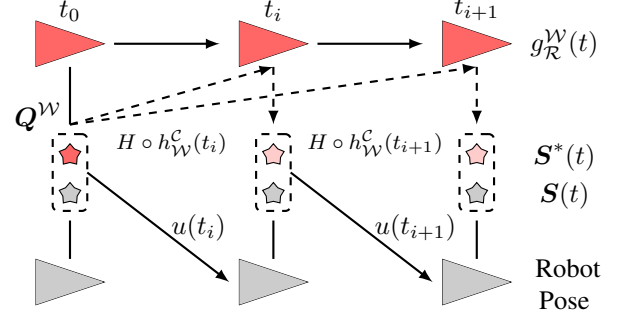


Fig. 3. Trajectory servoing process. Matches from S^* to S define the control u , where $S^*(t)$ is defined by the desired trajectory.

affect the feedback loop and further affect the control result. In addition, high visual processing latency will cause lower estimation accuracy due to late correction of raw IMU data [33]. To overcome these shortcomings, we design a mobile robot tracking method that bypasses pose feedback and provides feedback control directly through the image space.

The standard IBVS equations presented in §I-B typically apply to tracked features with known static positions in the world (relative to some frame attached to these positions). As described in §I-A.1 and §I-A.2, a visual map or visible targets are usually necessary. The prerequisites needed for stable tracking and depth recovery of features are major challenges regarding the use of visual servoing in unknown environments. Fortunately, they are all possible to meet based on information and modules available within the software stack of an autonomous mobile robot. This section describes the basic *trajectory servoing* implementation and describes how to build a solution that satisfies the prerequisites. It focuses on short-term navigation where sufficient image features remain within the field of view for the entire trajectory.

Trajectory servoing requirements condense down to the following: 1. A set of image points, $S^*(t_0)$, with known (relative) positions; 2. A given trajectory and control signal for the robot starting at the robot's current pose or nearby, $g_R^W(t_0)$; and 3. The ability to index and associate the image points across future image measurements, $S^*(t) \leftrightarrow S(t)$, when tracking the trajectory. The trajectory servoing process and variables are depicted in Fig. 3. The autonomy modules contributing this information are the navigation and V-SLAM stacks. The navigation stack generates a trajectory to follow. An indirect, feature-based V-SLAM stack will keep track of points in the local environment and link them to previously observed visual features while also estimating their actual position relative to the robot.

1) *Trajectory and control signals*: Define $\mathcal{S} = \{r_i\}_1^{n_F} \subset \mathbb{R}^2$ as a set of image points in the current camera image, sourced from the set $\mathcal{Q} = \{q_i^{\mathcal{W}}\}_1^{n_F} \subset \mathbb{R}^3$ of points in the world frame. Suppose that the robot should attain a future pose given by g^* , for which the points in \mathcal{Q} will project to the image coordinates $\mathcal{S}^* = H \circ (g^* h_C^{\mathcal{R}})^{-1}(\mathcal{Q})$. For simplicity, ignore field of view issues and occlusions between points. Their effect would be such that only a subset of the points in \mathcal{Q} would contribute to visual servoing.

Assume that a specific short-duration path has been established as the one to follow, and has been converted into a path relative to the robot's local frame. It either contains the current robot pose in it, or has a nearby pose. Contemporary navigation stacks have a means to synthesize both a time varying trajectory and an associated control signal from the paths. Here, we apply a standard trajectory tracking controller [37], to generate $\xi_u^*(t)$ and $g_{\mathcal{R}}^{\mathcal{W},*}(t)$ by forward simulating (1); note that ξ_u^* contains the linear velocity ν^* and angular velocity ω^* . Some navigation stacks use optimal control synthesis to build the trajectory. Either way, the generated trajectory is achievable by the robot.

In the time-varying trajectory tracking case, we assume that a trajectory reference $h_C^{\mathcal{W}}(t)$ exists along with a control signal $u^*(t)$ satisfying (2). It would typically be derived from a robot trajectory reference $g_{\mathcal{R}}^{\mathcal{W}}(t)$ and control signal $u^*(t)$ satisfying (1). Using those time-varying functions, the equations in (2) are solved to obtain the image coordinate trajectories. Written in short-hand to expose only the main variables, the forward integrated feature trajectory \mathcal{S}^* is:

$$\begin{aligned} \dot{\mathcal{S}}^* &= L \circ h_{\mathcal{W}}^{\mathcal{C}}(t)(\mathcal{Q}^{\mathcal{W}}) \cdot \zeta_{u^*(t)}, \text{ with} \\ \mathcal{S}^*(0) &= H \circ h_{\mathcal{W}}^{\mathcal{C}}(0)(\mathcal{Q}^{\mathcal{W}}). \end{aligned} \quad (6)$$

It will lead to a realizable visual servoing problem where ν^* , ω^* , and $\mathcal{S}^*(t)$ are consistent with each other. The equations will require converting the reference robot trajectory to a camera trajectory $h_C^{\mathcal{W},*}(t)$ using $\text{Ad}_{h_C^{\mathcal{R}}}^{-1}$.

2) *Features and feature paths*: The V-SLAM module provides a pool of visible features with known relative position for the current stereo frame, plus a means to assess future visibility if desired. Taking this pool to define the feature set $\mathcal{S}^*(0)$ gives the final piece of information needed to forward integrate (6) and generate feature trajectories $\mathcal{S}^*(t)$ in the left camera frame. This process acts like a short-term teach and repeat feature trajectory planner but is *simulate* and repeat, for on-the-fly generation of the repeat data.

A less involved module could be used besides a fully realized V-SLAM system, however doing so would require creating many of the fundamental building blocks of an indirect, feature-based V-SLAM system. Given the availability of strong performing open-source, real-time V-SLAM methods, there is little need to create a custom module. In addition, an extra benefit to tracked features through V-SLAM system is that a feature map is maintained to retrieve same reappeared features. As will be shown, this significantly improves the average lifetime of features, especially compared to a simple frame by frame tracking system without the feature map.

After the V-SLAM feature tracking process, we are already working with this feasible set whereby the indexed elements in \mathcal{S} correspond exactly to their counterpart in \mathcal{S}^* with the same index, i.e., the sets are *in correspondence*.

3) *Trajectory Servoing Control*: Define the error to be $\mathcal{E} = \mathcal{S} - \mathcal{S}^*$ where elements with matched indices are subtracted. The error dynamics of the points are:

$$\mathcal{E} = \dot{\mathcal{S}} - \dot{\mathcal{S}}^* = L_u(h_{\mathcal{W}}^{\mathcal{C}}(\mathcal{Q}), \mathcal{S}; h_{\mathcal{C}}^{\mathcal{R}}) \cdot u - \dot{\mathcal{S}}^* \quad (7)$$

where we apply the same argument adjustment as in (5) so that dependence is on image features then point coordinates as needed. Further, functions or operations applied to indexed sets will return an indexed set whose elements correspond to the input elements from the input indexed set. Since the desired image coordinates \mathcal{S}^* are not with respect to a static goal pose but a dynamic feature trajectory, $\dot{\mathcal{S}}^* \neq 0$, see (6). Define e , s , s^* , and L to be the vectorized versions of \mathcal{E} , \mathcal{S} , \mathcal{S}^* and L . Then,

$$\dot{e} = L(h_{\mathcal{W}}^{\mathcal{C}}(q), s; h_{\mathcal{C}}^{\mathcal{R}}) \cdot u - \dot{s}^* \quad (8)$$

is an overdetermined set of equations for u when $n_F > 2$. Removing the functional dependence and breaking apart the different control contributions, the objective is to satisfy,

$$\dot{e} = L \cdot u - \dot{s}^* = L^1 \nu + L^2 \omega - \dot{s}^* = -\lambda e. \quad (9)$$

A solution is to define,

$$\omega = (L^2)^{\dagger} (-L^1 \nu - \lambda e + \dot{s}^*), \quad (10)$$

so that

$$\dot{e} = -\lambda e + \Delta e, \quad (11)$$

where Δe is mismatch between the true solution and the computed pseudo-inverse solution. If the problem is realizable, then Δe will vanish and the robot will achieve the target pose. If Δe does not vanish, then there will be an error (usually some fixed point $e_{ss} \neq 0$). It is common for the robot's forward velocity to be set to a reasonable constant $\nu = \bar{\nu}$ in the angular control solution (9). This law drives the camera frame to the target pose (relative to \mathcal{W}).

Since the desired feature set is time varying from $\mathcal{S}^*(t)$ in equation (6):

$$\dot{s}^* = L^1(q^{C^*}(t), s^*(t))\nu^* + L^2(q^{C^*}(t), s^*(t))\omega^*. \quad (12)$$

The vectorized steering equations (10) lead to

$$\begin{aligned} \omega = (L^2(q^{\mathcal{C}}, s))^{\dagger} & \left(L^1(q^{C^*}(t), s^*(t))\nu^* - L^1(q^{\mathcal{C}}, s)\nu \right. \\ & \left. + L^2(q^{C^*}(t), s^*(t))\omega^* - \lambda e \right). \end{aligned} \quad (13)$$

They consist of feedforward terms derived from the desired trajectory and feedback terms to drive the error to zero. The feedforward terms should cancel out the $\dot{\mathcal{S}}^*$ term in (7), or equivalently the now non-vanishing \dot{s}^* term in (8). When traveling along the feature trajectory $\mathcal{S}^*(t)$, the angular velocity ω is computed from (13), where starred terms and ν are known quantities. To the best of our knowledge, no general IBVS tracking equations have been derived that combine feed-forward and feedback control elements.

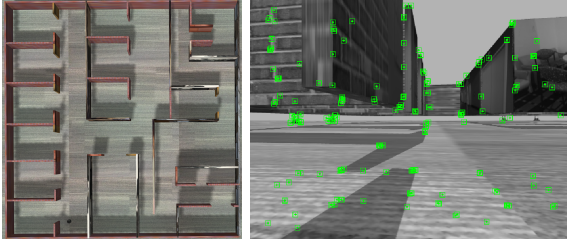


Fig. 4. Gazebo environment top view and robot view with SLAM features.

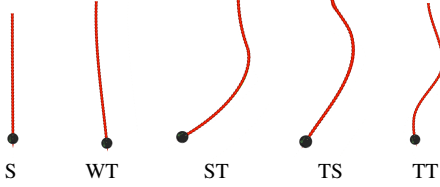


Fig. 5. Short-distance template trajectories.

C. Experiments and Results

This section runs several short distance trajectory servoing experiments to evaluate the accuracy of the image-based feedback strategy supplemented by stereo SLAM. The hypothesis is that mapping trajectory tracking to image-space will improve short term trajectory tracking by removing the impact of SLAM estimation drift from the feedback loop.

1) *Experimental Setup*: For quantifiable and reproducible outcomes, the ROS/Gazebo SLAM evaluation environment from [33] is used for the tests. Fig. 4 shows a top down view of the world plus a robot view. The simulated robot is a Turtlebot. It is tasked to follow a specific short-distance trajectory. A total of five paths were designed, loosely based on Dubins paths. They are denoted as straight (S), weak turn (WT), straight+turn (ST), turn+straight (TS), turn+turn (TT), and are depicted in Fig. 5. Average length of all trajectories are $\sim 4\text{m}$. Longer paths would consist of multiple short segment reflecting variations on this path set. They are designed to ensure that sufficient feature points visible in the first frame remain visible along the entirety of the path. Five trials per trajectory are run. The desired and actual robot poses are recorded for performance scoring. Performance metrics computed are average translation error (ATE).

2) *SLAM Stack*: Part of the robot's software stack includes the Good Feature (GF) ORB-SLAM system [25] for estimating camera poses. It is configured to work with a stereo camera and integrated into a loosely coupled, visual-inertial (VI) system [33], [38] based on a multi-rate filter to form a VI-SLAM system. The trajectory servoing system will interface with the GF-ORB-SLAM system to have access to tracked features for IBVS.

3) *Methods Tested*: In addition to the trajectory servoing algorithm, several baseline methods are implemented. The first is a pose feedback strategy using *perfect odometry* (PO) as obtained from the actual robot pose in the Gazebo simulator. The second replaced PO with the SLAM estimated pose, which are delayed and have uncertainty. The third is a trajectory servoing method without the V-SLAM system, which would be a naive implementation of visual servoing based on (13). It is called VS+ to differentiate from trajectory

servoing, and uses a frame-by-frame stereo feature tracking system [39]. Pose-based control [33] uses a geometric trajectory tracking controller with feedforward $[\nu^*, \omega^*]^T$ and feedback

$$\begin{aligned} \nu_{cmd} &= k_x * \tilde{x} + \nu^* \\ w_{cmd} &= k_\theta * \tilde{\theta} + k_y * \tilde{y} + \omega^* \end{aligned} \quad (14)$$

where,

$$[\tilde{x}, \tilde{y}, \tilde{\theta}]^T \simeq \tilde{g} = g^{-1} g^* = (g_{\mathcal{R}}^{\mathcal{W}})^{-1}(t) (g_{\mathcal{R}}^{\mathcal{W},*})(t). \quad (15)$$

The controller gains have been empirically tuned to give good performance for the perfect odometry case, and have been extensively used in prior work [1], [2], [33].

4) *Results and Analysis*: Tables I to IV quantify the outcomes of all methods tested. Fig. 6 consists of boxplots of the trajectory tracking error for the different template trajectories and methods (minus VS+). The first outcome to note is that VS+ fails for all paths. The average length of successful servoing is 0.4m ($\sim 10\%$ of the path length). Inconsistent data association rapidly degrades the feature pool and prevents consistent use of feature for servoing feedback. Without the feature map in V-SLAM, a reappeared feature will be treated as a new feature and assigned with a different index, which easily violates the *correspondence* rule from §II-B.2. As noted there, any effort to improve this would increasingly approach the computations found in a V-SLAM method. Maintaining stable feature tracking through V-SLAM is critical to trajectory servoing.

Comparing SLAM and TS, the Table values show lower errors across the board, and lower control cost. Trajectory tracking error is lower by 71% and terminal error is lower by 44%. Interestingly, the pose estimation error is only reduced by around 12%, which indicates weak improvement in pose estimation from the better tracking via TS. This is most likely a result of the SLAM pose predictions being decoupled from the control system, leading to uninformed motion priors. ORB-SLAM uses a motion prior based on its own internal estimates. Tightly coupling the two parts may improve the SLAM system, but may also introduce new sensitivities. The TS approach reduces control effort by 19%.

Comparing PO with TS shows better performance by TS, which was not expected. This might suggest some additional tuning would be necessary. However, usually there is trade-off between tracking error and control cost. Attempts to improve tracking usually increase the control cost, and vice-versa. Based on the values of the Tables, it is not clear that better would be possible. Tests later in this manuscript will show that the benefit does not persist for longer paths, thus the improvement for short trajectories is of limited use. The finding here is that implementing a purely image-based approach to trajectory tracking through unknown environments is possible, and can work well over short segments in the absence of global positioning information.

III. LONG DISTANCE TRAJECTORY SERVOING

Short-term trajectory servoing cannot extend to long trajectories due to feature impoverishment. When moving

TABLE I
TRAJECTORY TRACKING ATE (CM)

Seq.	PO	SLAM	TS	VS+
S	2.27	3.67	0.76	x
WT	1.62	3.62	0.76	x
ST	2.50	2.96	1.06	x
TS	1.58	3.24	1.33	x
TT	2.35	3.50	1.04	x
Avg. ATE	2.06	3.40	0.99	x

TABLE II
TERMINAL ERROR (CM)

Seq.	PO	SLAM	TS
S	2.47	5.44	1.29
WT	1.83	5.93	1.30
ST	2.85	1.50	2.99
TS	1.85	1.76	2.04
TT	2.34	3.07	2.27
Avg.	2.27	3.54	1.98

TABLE III
ESTIMATION ATE (CM)

Seq.	SLAM	TS
S	1.16	1.41
WT	1.63	1.66
ST	2.48	3.00
TS	4.22	3.91
TT	3.75	3.36
Avg.	3.02	2.67

TABLE IV
CONTROL EFFORT

Seq.	PO		SLAM		TS	
•	ν	ω	ν	ω	ν	ω
S	7.88	0.20	7.10	0.19	5.86	1.17
WT	8.14	0.55	7.35	0.48	6.16	1.84
ST	7.58	4.73	6.70	3.47	5.67	3.38
TS	8.18	4.92	7.33	4.27	6.19	4.46
TT	8.47	4.82	7.72	4.24	6.46	4.75
Avg.	8.05	3.04	7.24	2.53	6.07	3.12
•	11.09		9.77		9.19	

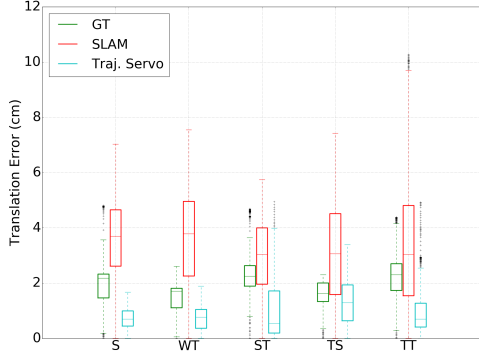


Fig. 6. Short-distance trajectory benchmarking results

beyond the initially visible scene, a more comprehensive trajectory servoing system would augment the feature pool \mathcal{S}^* with new features. Likewise, if navigation consists of multiple short distance trajectories, then the system must have a regeneration mechanism for synthesizing entirely new desired feature tracks for the new segment. The overlapping needs for these two events inform the creation of a module for feature replenishment and trajectory extension.

A. Feature Replenishment

The number of feature correspondences n_F in \mathcal{S} and \mathcal{S}^* indicates whether trajectory servoing can be performed without concern. Let the threshold τ_{fr} determine when feature replenishment should be triggered. Define $\mathcal{S}_i^*(t)|_{t_{i,s}}^{t_{i,e}}$ as the i^{th} feature trajectory starting from $t_{i,s}$ and ending at $t_{i,e}$. The case $i = 0$ represents the first feature trajectory segment generated by (6) for $t_{i,s} = 0$, integrated up to the maximum time t_{end} of the given trajectory. The time varying function $n_F(t)$ is the actual number of feature correspondences between $\mathcal{S}(t)$ and $\mathcal{S}_i^*(t)$ as the robot proceeds.

When $n_F(t) \geq \tau_{fr}$, the feature trajectory $\mathcal{S}_i^*(t)$ may be used for trajectory servoing. When $n_F(t) < \tau_{fr}$, the feature replenishment process will be triggered at the current time and noted as $t_{i,e}$. The old feature trajectory $\mathcal{S}_i^*(t)|_{t_{i,s}}^{t_{i,e}}$ is finished. A new feature trajectory is generated with

$$\mathcal{S}_{i+1}^*(t)|_{t_{i+1,s}}^{t_{i+1,e}} = H \circ (g^*(t_{i,e}, t) h_C^R)^{-1} (Q^W(t_{i,e})), \quad (16)$$

where $g^*(t_{i,e}, t)$ is the transformation between the current robot pose and a future desired pose ($t > t_{i,e}$) on the trajectory. The poses behind the robot are not included. The set $Q^W(t_{i,e})$ consists of observed points at the current time $t_{i,e}$. The feature pool is augmented by these current features. When this regeneration step is finished, the exact time will be

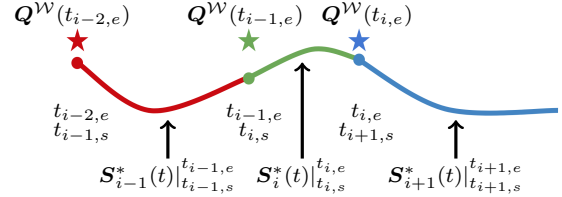


Fig. 7. Feature replenishment process. There are three segments of feature trajectories. Stars are observed point sets at corresponding time. Each circle is the start or end time of next or this segment of feature trajectory. Three feature trajectories are generated by the feature replenishment equation (16).

assigned as the $t_{i+1,s}$. Trajectory servoing is performed on this new feature trajectory until the regeneration is triggered again or the arriving at the end of the trajectory. The process of regenerating new feature tracks is equivalent to dividing a long trajectory into a set of shorter segments pertaining to the generated feature trajectory segments. An example of this feature replenishment is shown in Fig. 7.

During navigation, (16) requires the current robot pose relative to the initial pose to be known. In the absence of an absolute reference or position measurement system, the only option available is to use the estimated robot pose from V-SLAM, or some equivalent process. Although there are some drawbacks to relying on V-SLAM, it attempts to keep pose estimation as accurate as possible over long periods through feature mapping, bundle adjustment, loop closure, etc.. To further couple V-SLAM and trajectory servoing, we design a multi-loop scheme, see Fig. 8. The inner loop is governed by trajectory servoing with V-SLAM tracked features. The V-SLAM estimated pose will only be explicitly used in the outer loop when performing feature replenishment. In this way, the inner visual feedback loop will not be affected by the uncertainty from pose estimation. Plus the outer loop will only be activated when starting a new feature replenishment; and since the visual information is received, fused, and optimized with an IMU, it generates a robot pose that is more reliable than the raw poses used in the inner loop of V-SLAM pose based control (shown in Fig. 2). However, relying on V-SLAM still introduces measurement error or drift, which means that long-term trajectory servoing along an absolute, desired trajectory will accrue error.

B. Experiments and Results

This section modifies the experiments in §II-C to involve longer trajectories that will trigger feature replenishment

TABLE V
TRACKING ATE (CM)

Seq.	PO	SLAM	TS
RU	2.40	6.19	4.02
LU	3.47	17.22	7.30
ST	2.25	7.95	6.06
ZZ	5.19	11.01	8.30
Avg. ATE	3.33	10.59	6.42

TABLE VI
TERMINAL ERROR (CM)

Seq.	PO	SLAM	TS
RU	2.33	11.61	6.77
LU	3.14	26.06	18.90
ST	2.38	8.61	7.74
ZZ	4.28	5.22	7.18
Avg.	3.03	12.88	10.15

TABLE VII
ESTIMATION ATE (CM)

Seq.	SLAM	TS
RU	9.15	8.49
LU	13.68	11.09
ST	7.00	7.96
ZZ	12.13	10.37
Avg.	10.49	9.48

TABLE VIII
CONTROL EFFORT

Seq.	PO		SLAM		TS	
•	ν	ω	ν	ω	ν	ω
RU	15.51	14.95	13.94	12.08	11.94	10.80
LU	17.77	9.53	16.38	9.24	13.67	9.94
ST	17.80	13.87	16.00	12.96	13.74	12.29
ZZ	23.17	11.73	21.00	10.67	17.97	10.89
Avg.	18.56	12.52	16.83	11.24	14.33	10.98
•	31.08		28.07		25.31	

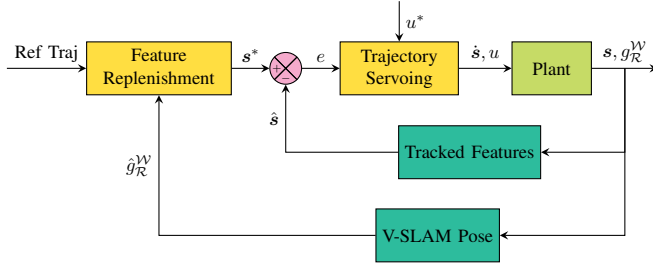


Fig. 8. Block Diagram for long-term Trajectory Servoing

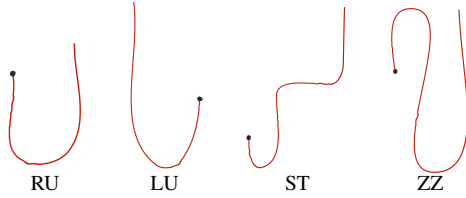


Fig. 9. Long-distance trajectories

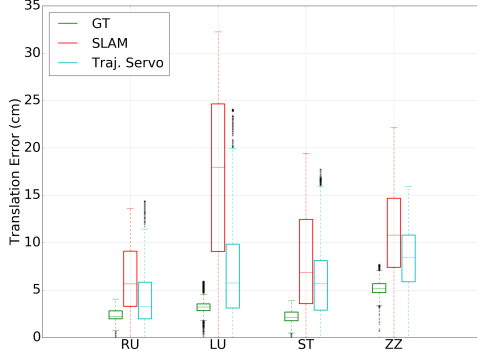


Fig. 10. Long trajectory benchmarking results

and synthesize new feature trajectory segments. The set of trajectories to track is depicted in Fig. 9. They are denoted as right u-turn (RU), left u-turn (LU), straight+turn (ST), and zig-zag (ZZ). Each trajectory is longer than 20m. Testing and evaluation follows as before (minus VS+).

1) *Results and Analysis:* Fig. 10 consists of boxplots of the translation-only trajectory tracking ATE for the template trajectories. As hypothesized, the error over longer trajectories is affected by the need to use SLAM pose estimates for regeneration. The PO method outperforms TS, but TS still operates better than SLAM. However, it appears that in the one case where the SLAM system performed the worst, the TS approach had better performance. The tabulated results in Tab. V and VI indicates that on average the TS approach improved over SLAM by 39% and 21% in terms of tracking error and terminal error. What is interesting is that the

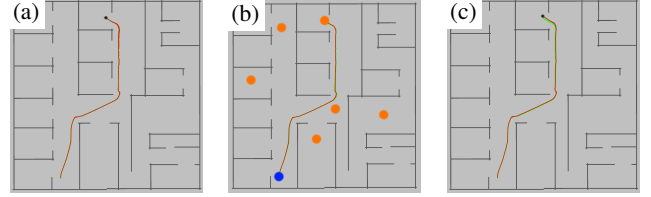


Fig. 11. Navigation with global planning. Blue point is the robot starting position. Orange points are 6 goal points for navigation. In each figure, green is the collision-free global path. Red is the real robot trajectory overlaying on the green trajectory. The figures show successful navigation examples of the same goal point with three different controllers. (a) Pose-based trajectory tracking with perfect odometry. (b) Vision-based trajectory tracking. (c) Pose-based trajectory tracking with estimated poses from V-SLAM. It can be observed that the red trajectory has less deviations from the green trajectory with TS (b) than SLAM (c).

estimation ATE of both systems is comparable (Tab. VII), which indicates that trajectory servoing may have better closed-loop noise rejection properties by working directly in image-space instead of using inferred pose estimates from the SLAM estimator. Tab. VIII suggests that control efforts of both ν and ω are the lowest. The combined control effort of TS is reduced 19% and 10% from PO and SLAM. That TS may change the performance vs. cost trade-off curves should be studied further.

C. Navigation with online path planning

To show how trajectory servoing works for a navigation task, we move the environment down to the ground and create a 2D occupancy map. Given a goal, the global planner identifies a feasible collision-free path from the map. The online global path is used for the robot to apply trajectory servoing. The full system in Fig. 1 is used. Fig. 11 shows one successful navigation task for three tracking methods. The robot starts from the blue point, and ends at 6 different positions, marked as orange points. The average ATE for PO, SLAM and TS are 1.31cm, 7.39cm and 7.30cm. And the average terminal errors are 1.46cm, 14.49cm and 13.13cm. Trajectory servoing, enabled by V-SLAM, has better performance than using V-SLAM for pose-based feedback. The smaller performance gap between TS and SLAM for these navigation tasks requires further investigation. Per Tables III and VII, it appears to be dependent on SLAM estimation error, as the gap is close to the estimation gap ($\sim 10\%$). There may be a mechanism to better estimate motion from the initial pose to the terminal pose of a trajectory segment, which might involve more tightly coupling the short distance module with the SLAM module (see Fig. 1).

IV. CONCLUSION

In the paper, we presented a vision-based navigation approach for a non-holonomic mobile ground robot called *trajectory servoing*, which combines the IBVS and V-SLAM. This trajectory tracking method can successfully follow a given short trajectory without externally derived robot pose information. By integrating with estimated robot poses from V-SLAM, it can achieve long-term navigation. The V-SLAM system also provides robust feature tracking to support stable trajectory servoing. Experiments demonstrated improved tracking accuracy over pose-based trajectory tracking using estimated SLAM poses.

Future work intends to implement trajectory servoing approach on a real Turtlebot platform to evaluate its performance. We also plan to perform uncertainty analysis on the trajectory servoing feedback equations to provide robustness to real-world measurement errors, which will also aid in matching simulation performance outcomes to actual performance.

REFERENCES

- [1] J. S. Smith and P. A. Vela, "PiPS: Planning in perception space," in *ICRA*, May 2017, pp. 6204–6209.
- [2] J. S. Smith, S. Feng, F. Lyu, and P. A. Vela, *Real-Time Egocentric Navigation Using 3D Sensing*. Cham: Springer International Publishing, 2020, pp. 431–484.
- [3] S. Šegvić, A. Remazeilles, A. Diosi, and F. Chaumette, "A mapping and localization framework for scalable appearance-based navigation," *CVIU*, vol. 113, no. 2, pp. 172 – 187, 2009.
- [4] T. Krajník, F. Majer, L. Halodová, and T. Vintr, "Navigation without localisation: reliable teach and repeat based on the convergence theorem," in *IROS*, 2018, pp. 1657–1664.
- [5] L. Halodová, E. Dvořáková, F. Majer, T. Vintr, O. M. Mozos, F. Dayoub, and T. Krajník, "Predictive and adaptive maps for long-term visual navigation in changing environments," in *IROS*, 2019, pp. 7033–7039.
- [6] T. Do, L. C. Carrillo-Arce, and S. I. Roumeliotis, "High-speed autonomous quadrotor navigation through visual and inertial paths," *IJRR*, vol. 38, no. 4, pp. 486–504, 2019.
- [7] P. Furgale and T. Barfoot, "Visual teach and repeat for long-range rover autonomy," *J. Field Robot.*, vol. 27, pp. 534–560, 09 2010.
- [8] T. Krajník, P. Cristóforis, K. Kusumam, P. Neubert, and T. Duckett, "Image features for visual teach-and-repeat navigation in changing environments," *Robotics and Autonomous Systems*, vol. 88, pp. 127 – 141, 2017.
- [9] N. Zhang, M. Warren, and T. D. Barfoot, "Learning place-and-time-dependent binary descriptors for long-term visual localization," in *ICRA*, 2018, pp. 828–835.
- [10] T. Nguyen, G. K. Mann, R. G. Gosine, and A. Vardy, "Appearance-based visual-teach-and-repeat navigation technique for micro aerial vehicle," *J. Intell. Robotics Syst.*, vol. 84, no. 1–4, p. 217–240, Dec. 2016.
- [11] K. Kidono, J. Miura, and Y. Shirai, "Autonomous visual navigation of a mobile robot using a human-guided experience," *Robotics and Autonomous Systems*, vol. 40, no. 2, pp. 121 – 130, 2002.
- [12] A. Pfrunder, A. P. Schoellig, and T. D. Barfoot, "A proof-of-concept demonstration of visual teach and repeat on a quadcopter using an altitude sensor and a monocular camera," in *Canadian Conference on Computer and Robot Vision*, 2014, pp. 238–245.
- [13] A. Vardy, "Using feature scale change for robot localization along a route," in *IROS*, 2010, pp. 4830–4835.
- [14] N. M. Garcia and E. Mails, "Preserving the continuity of visual servoing despite changing image features," in *IROS*, vol. 2, 2004, pp. 1383–1388 vol.2.
- [15] F. Chaumette and S. Hutchinson, "Visual servo control. I. basic approaches," *RAM*, vol. 13, no. 4, pp. 82–90, 2006.
- [16] —, "Visual servo control. II. advanced approaches," *RAM*, vol. 14, no. 1, pp. 109–118, 2007.
- [17] Y. Mezouar and F. Chaumette, "Path planning for robust image-based control," *IEEE Transactions on Robotics and Automation*, vol. 18, no. 4, pp. 534–549, 2002.
- [18] F. Fahimi and K. Thakur, "An alternative closed-loop vision-based control approach for unmanned aircraft systems with application to a quadrotor," in *ICUAS*, 2013, pp. 353–358.
- [19] A. Cherubini, F. Chaumette, and G. Oriolo, "Visual servoing for path reaching with nonholonomic robots," *Robotica*, vol. 29, no. 7, pp. 1037–1048, 2011.
- [20] A. Ahmadi, L. Nardi, N. Chebrolu, and C. Stachniss, "Visual servoing-based navigation for monitoring row-crop fields," in *ICRA*, May 2020, pp. 4920–4926.
- [21] A. Remazeilles, F. Chaumette, and P. Gros, "3d navigation based on a visual memory," in *ICRA*, 2006, pp. 2719–2725.
- [22] A. Diosi, S. Segvic, A. Remazeilles, and F. Chaumette, "Experimental evaluation of autonomous driving based on visual memory and image-based visual servoing," *T-ITS*, vol. 12, no. 3, pp. 870–883, 2011.
- [23] G. Blanc, Y. Mezouar, and P. Martinet, "Indoor navigation of a wheeled mobile robot along visual routes," in *ICRA*, 2005, pp. 3354–3359.
- [24] C. Cadena, L. Carlone, H. Carrillo, Y. Latif, D. Scaramuzza, J. Neira, I. Reid, and J. J. Leonard, "Past, present, and future of simultaneous localization and mapping: Toward the robust-perception age," *T-RO*, vol. 32, no. 6, pp. 1309–1332, 2016.
- [25] Y. Zhao and P. A. Vela, "Good feature matching: Toward accurate, robust vo/vslam with low latency," *T-RO*, vol. 36, no. 3, pp. 657–675, 2020.
- [26] L. Nardi, B. Bodin, M. Z. Zia, J. Mawer, A. Nisbet, P. H. J. Kelly, A. J. Davison, M. Luján, M. F. P. O'Boyle, G. Riley, N. Topham, and S. Furber, "Introducing slambench, a performance and accuracy benchmarking methodology for slam," in *ICRA*, 2015, pp. 5783–5790.
- [27] S. Saeedi, B. Bodin, H. Wagstaff, A. Nisbet, L. Nardi, J. Mawer, N. Melot, O. Palomar, E. Vespa, T. Spink, C. Gorgovan, A. Webb, J. Clarkson, E. Tomusk, T. Debrunner, K. Kaszyk, P. Gonzalez-De-Aledo, A. Rodchenko, G. Riley, C. Kotselidis, B. Franke, M. F. P. O'Boyle, A. J. Davison, P. H. J. Kelly, M. Luján, and S. Furber, "Navigating the landscape for real-time localization and mapping for robotics and virtual and augmented reality," *Proceedings of the IEEE*, vol. 106, no. 11, pp. 2020–2039, 2018.
- [28] M. Bujanca, P. Gafton, S. Saeedi, A. Nisbet, B. Bodin, M. F. P. O'Boyle, A. J. Davison, P. H. J. Kelly, G. Riley, B. Lennox, M. Luján, and S. Furber, "Slambench 3.0: Systematic automated reproducible evaluation of slam systems for robot vision challenges and scene understanding," in *ICRA*, 2019, pp. 6351–6358.
- [29] J. Delmerico and D. Scaramuzza, "A benchmark comparison of monocular visual-inertial odometry algorithms for flying robots," in *ICRA*, 2018, pp. 2502–2509.
- [30] I. Cvišić, J. Česić, I. Marković, and I. Petrović, "Soft-SLAM: Computationally efficient stereo visual simultaneous localization and mapping for autonomous unmanned aerial vehicles," *J. Field Robot.*, vol. 35, no. 4, pp. 578–595, 2018.
- [31] A. Weinstein, A. Cho, G. Loianno, and V. Kumar, "Visual inertial odometry swarm: An autonomous swarm of vision-based quadrotors," *RA-L*, vol. 3, no. 3, pp. 1801–1807, 2018.
- [32] Y. Lin, F. Gao, T. Qin, W. Gao, T. Liu, W. Wu, Z. Yang, and S. Shen, "Autonomous aerial navigation using monocular visual-inertial fusion," *J. Field Robot.*, vol. 35, no. 1, pp. 23–51, 2018.
- [33] Y. Zhao, J. S. Smith, S. H. Karumanchi, and P. A. Vela, "Closed-loop benchmarking of stereo visual-inertial SLAM systems: Understanding the impact of drift and latency on tracking accuracy," *ICRA*, pp. 1105–1112, 2020.
- [34] S. Hutchinson, G. D. Hager, and P. I. Corke, "A tutorial on visual servo control," *IEEE Transactions on Robotics and Automation*, vol. 12, no. 5, pp. 651–670, 1996.
- [35] R. Murray, Z. Li, and S. Sastry, *A Mathematical Introduction to Robotic Manipulation*. CRC Press, 1994.
- [36] H. Liu, R. Jiang, W. Hu, and S. Wang, "Navigational drift analysis for visual odometry," *Comput. Informatics*, vol. 33, pp. 685–706, 2014.
- [37] R. Olfati-Saber, "Near-identity diffeomorphisms and exponential ϵ -tracking and ϵ -stabilization of first-order nonholonomic SE(2) vehicles," in *ACC*, vol. 6, May 2002, pp. 4690–4695 vol.6.
- [38] S. M. Weiss, "Vision based navigation for micro helicopters," Ph.D. dissertation, ETH Zurich, Zürich, 2012.
- [39] S. Feng, (2020) Frame-by-frame stereo feature tracking system.

[Online]. Available: <https://github.com/ivaROS/stereoFeatureTracking.git>